Springer

KSME

Journal of Mechanical Science and Technology 26 (6) (2012) 1901~1909
www.springerlink.com/content/1738-494x
DOI 10.1007/s12206-012-0408-5

A novel six-degrees-of-freedom series-parallel manipulator †

J. Gallardo-Alvarado*, R. Rodríguez-Castro, C. R. Aguilar-Nájera and L. Pérez-González

Department of Mechanical Engineering, Instituto Tecnológico de Celaya, Celaya, GTO, México

(Manuscript Received May 26, 2011; Revised September 29, 2011; Accepted January 27, 2012)

Abstract

This paper addresses the description and kinematic analyses of a new non-redundant series-parallel manipulator. The primary feature of the robot is to have a decoupled topology consisting of a lower parallel manipulator, for controlling the orientation of the coupler platform, assembled in series connection with a upper parallel manipulator, for controlling the position of the output platform, capable to provide arbitrary poses to the output platform with respect to the fixed platform. The forward displacement analysis is carried-out in semi-closed form solutions by resorting to simple closure equations. On the other hand; the velocity, acceleration and singularity analyses of the manipulator are approached by means of the theory of screws. Simple and compact expressions are derived here for solving the infinitesimal kinematics by taking advantage of the concept of reciprocal screws. Furthermore, the analysis of the Jacobians of the robot shows that the lower parallel manipulator is practically free of singularities. In order to illustrate the performance of the manipulator, a numerical example which consists of solving the inverse/forward kinematics of the series-parallel manipulator as well as its singular configurations is provided.

Keywords: Parallel manipulator; Compliant orientation; Compliant translation; Screw theory; Kinematics

1. Introduction

A series-parallel manipulator, term proposed by Zoppi et al. [1], is a mechanism composed by two parallel manipulators assembled in series connection, and represents a viable option to overcome the complex forward kinematics of the Gough-Stewart platform [2]. In fact, while the forward displacement analysis of the general hexapod yields a 40-th univariate polynomial equation [3, 4], which implies a high computational complexity, all solutions of the same analysis stem from two 8-th univariate polynomial equations, see for instance Gallardo-Alvarado et al. [5], for most series-parallel manipulators. The series-parallel manipulator proposed in this work is inspired on the well-known 3-RPS parallel manipulator, where R, P and S stand for revolute, prismatic, and spherical joints, respectively. The 3-RPS robot belongs to the class known as zero-torsion mechanisms [6, 7] and its mobility was investigated by means of the theory of screws by Dai et al. [8]. This limited-dof parallel manipulator was introduced almost three decades ago by Hunt [9] and even though its limited mobility, two rotations plus one translation, it has been the motive of an exhaustive and fruitful research field which can be used, as it is proposed by Waldron et al. [10], as part of a series-parallel manipulator. Other applications include micromotion parallel manipulators [11], biomechanical devices like the ankle [12], multi-axis manufacturing cells [13], partially decoupled robots [14, 15], the development of a class of hyper-redundant manipulators [16, 17] and so on.

On the other hand, it is interesting to note that a series-parallel manipulator with different performance can be obtained by changing the sequence of its kinematic pairs. In that way Lu et al. [18] approached the kinematics and statics of an inversion of the 2(3-RPS) robot.

This work introduces a new six-degrees-of-freedom non-redundant spatial series-parallel manipulator, in other words a robot where the number of degrees of freedom is equal to the six-dimensional task space. Naturally the number of available motors or generalized coordinates is also equal to the degrees of freedom of the proposed robot.

2. Description of the robot

The proposed robot, see Fig. 1, consists of a lower parallel manipulator (LPM) and an upper parallel manipulator (UPM) connected to each other through *'compound joints'* attached to a coupler platform (body 2). A compound joint results from the combined action of a revolute joint covering a spherical joint where the revolute axis intersects the center of the spherical joint.

The LPM is a 3-PPS parallel manipulator where the kinematic pairs connecting the limbs to the fixed platform (body

*Corresponding author. Tel.: +52 461 6117575, Fax.: +52 461 6117979
E-mail address: gjaime@itc.mx
† Recommended by Associate Editor Yang Shi

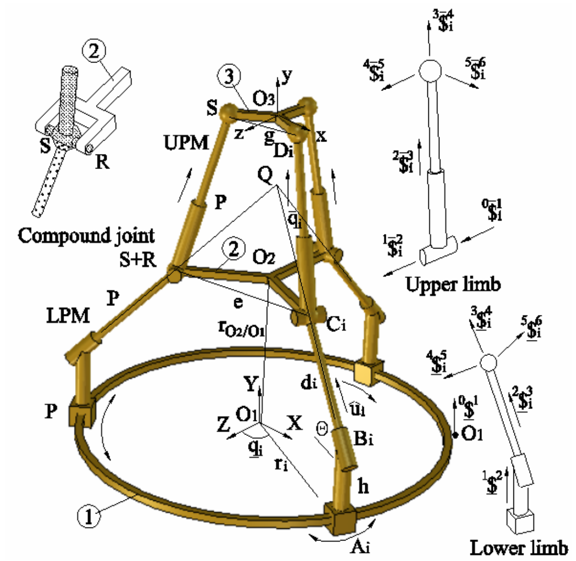

Fig. 1. The proposed series-parallel manipulator.

1) are circular-prismatic joints, which can also be simulated as revolute joints, while the UPM is a 3-RPS parallel manipulator containing the output platform (body 3) of the robot. The revolute joints mounted on the coupler platform have a tangential arrangement shaping an equilateral triangle of side *e*, whereas another equilateral triangle of side *g* is formed with the centers of the spherical joints mounted on the output platform. Lower links of length *h* move on circular trajectories of radius *r* about the center O_1 of the fixed platform. Furthermore, each lower link is connected to the coupler platform by means of an inclined PS-type kinematic chain where the angle Θ, measured from the plane of the fixed platform to the variable rod, is the same for the three PS limbs which implies that the lines along them intersect a common point Q. The proposed series-parallel manipulator, using the Chebychev-Grübler-Kutzbach criterion [19], is capable to realize six degrees of freedom which are explained as follows. The LPM can be treated as a modification of the 3-RPS parallel manipulator where the moving platform, here called coupler platform, can undergo arbitrary orientations followed by parasitic translations, an unusual application of a zero-torsion parallel manipulator. The LPM is similar to the 3-RRPS six-degrees-of-freedom parallel manipulator investigated in Alizade et al. [20] where each of its limbs is a mechanical generator. However the reduction of kinematic pairs and the arrangement of revolute joints with collinear axes intersecting a common point in order to generate a subgroup of the Euclidean group *E*(3) is a novel proposition of the contribution. On the other hand, the UPM is a classical 3-RPS tangential parallel manipulator whose moving platform, hereafter called output platform, can undergo arbitrary displacements accomplished by parasitic rotations. Therefore it is evident that the orientation and position of the output platform, with respect to the fixed platform, of the series-parallel manipulator under study are controlled, respectively, by means of the lower and upper parallel manipulators. The concept is simple but effective, (arbitrary orientation + parasitic translation) + (arbitrary displacement + parasitic orientation) = series-parallel manipulator with decoupled kinematics.

3. Finite kinematics of the robot

Let *XYZ* be a reference frame attached at the center O_1 of the fixed platform, and let *xyz* be a moving reference frame attached at the center O_3 of the output platform. The forward position analysis of the proposed mechanism is formulated as follows: given the generalized coordinates $\{\underline{q}_i, \overline{q}_i\}$, in the remainder of the contribution *i* = 1, 2, 3; compute the pose of the output platform with respect to the fixed platform. A strategy to approach this analysis consists of determining firstly the coordinates of the centers C_i of the spherical joints attached at the coupler platform. To this end, consider that the position vectors $\boldsymbol{C}_i$ of such points can be obtained, see Fig. 1, as

$$\boldsymbol{C}_i = \boldsymbol{A}_i + \boldsymbol{h} + d_i \hat{\boldsymbol{u}}_i \tag{1}$$

where $\boldsymbol{A}_i = \mathbf{r}_i = r\sin(\underline{q}_i)\hat{i} + r\sin(\underline{q}_i)\hat{k}$ is the position vector of the nominal point A_i of the i-th lower link, $\boldsymbol{h} = h\hat{j}$ and $\hat{\boldsymbol{u}}_i = -\cos(\Theta)\sin(\underline{q}_i)\hat{i} + \sin(\Theta)\hat{j} - \cos(\Theta)\cos(\underline{q}_i)\hat{k}$ is the unit vector along the i-th PS kinematic chain. Clearly, nine linear equations in twelve unknowns can be obtained upon expressions (1). In order to complete the number of equations, consider that the equilateral triangle $\Delta C_1C_2C_3$ brings three non-linear equations as follows:

$$(\boldsymbol{C}_i - \boldsymbol{C}_j) \bullet (\boldsymbol{C}_i - \boldsymbol{C}_j) = e^2 \quad i, j = 1, 2, 3 \mod(3) \tag{2}$$

where the dot (•) denotes the inner product of the usual three-dimensional vectorial algebra. After a few computations, Eqs. (1) and (2) are reduced into a non-linear system of three equations in the unknowns d_i as

$$K_1^i d_i^2 + K_2^i d_j^2 + K_3^i d_i d_j + K_4^i d_i + K_5^i d_j + K_6^i = 0 \quad i, j = 1, 2, 3 \mod(3) \tag{3}$$

where the coefficients $K_j^i \ (j = 1, 2, \ldots, 6)$ are computed according to the lower generalized coordinates $\underline{q}_i$ and parameters of the mechanism. Expressions (3) are called the *characteristic equations of the LPM*. A systematic application of the Sylvester dialytic elimination method allows obtaining an 8-th univariate polynomial equation upon expressions (3) which indicates that the coupler platform can reach at most eight distinct poses with respect to the fixed platform. Once the coordinates of the centers C_i of the lower spherical joints are computed, solving Eqs. (3) and (1), the position vector $\boldsymbol{r}_{O_2/O_1}$ of the center of the coupler platform expressed in the reference frame *XYZ* results in

$$\boldsymbol{r}_{O_2/O_1} = (\boldsymbol{C}_1 + \boldsymbol{C}_2 + \boldsymbol{C}_3)/3 . \tag{4}$$

In what follows the coordinates of the centers of the spherical joints attached at the output platform, points D_i located by vectors $\boldsymbol{D}_i$, will be computed. To this end, due to the tangential arrangement of the revolute joints mounted on the coupler platform it is possible to write

$$(\boldsymbol{C}_i - \boldsymbol{C}_j)\bullet(\boldsymbol{D}_k - \boldsymbol{C}_k) = 0 \;\; i,j,k = 1,2,3 \;\; \text{mod}(3) . \tag{5}$$

Furthermore, it is evident that the variable-length rods $\overline{q}_i$ must satisfy

$$(\boldsymbol{D}_i - \boldsymbol{C}_i)\bullet(\boldsymbol{D}_i - \boldsymbol{C}_i) = \overline{q}_i^2 . \tag{6}$$

Finally, the equilateral triangle $\Delta D_1D_2D_3$ yields three compatibility kinematic constraint equations as

$$(\boldsymbol{D}_i - \boldsymbol{D}_j)\bullet(\boldsymbol{D}_i - \boldsymbol{D}_j) = g^2 \;\; i,j = 1,2,3 \;\; \text{mod}(3) . \tag{7}$$

The solution of the Eqs. (5)-(7) is a well-known mathematical procedure, see for instance Innocenti and Parenti-Castelli [21], and therefore it is unnecessary to include it here. Once the coordinates of points D_i are calculated, the pose of the output platform, with respect to the fixed platform, can be considered as the homogeneous transformation matrix ${}^1\mathbf{T}^3$ given by

$${}^1\mathbf{T}^3 = \begin{bmatrix} {}^1\mathbf{R}^3 & \boldsymbol{r}_{O_3/O_1} \\ 0 & 1 \end{bmatrix} \tag{8}$$

where the rotation matrix ${}^1\mathbf{R}^3$ can be easily computed using the method introduced in Gallardo-Alvarado et al. [17], while the position vector $\boldsymbol{r}_{O_3/O_1}$ of the center of the output platform, with respect to the fixed platform, is given by

$$\boldsymbol{r}_{O_3/O_1} = (\boldsymbol{D}_1 + \boldsymbol{D}_2 + \boldsymbol{D}_3)/3 . \tag{9}$$

On the other hand, the inverse position analysis consists of finding the generalized coordinates $\{\underline{q}_i, \overline{q}_i\}$ given the pose of the output platform with respect to the fixed platform, in other words given the rotation matrix ${}^1\mathbf{R}^3$ and the position vector $\boldsymbol{r}_{O_3/O_1}$.

Using classical roll (γ), pitch (β) and yaw (α) angles, the rotation matrix ${}^1\mathbf{R}^3_{\gamma\beta\alpha}$ between the output and fixed platforms is given by

$${}^1\mathbf{R}^3_{\gamma\beta\alpha} = \begin{bmatrix} c\alpha c\beta & c\alpha s\beta s\gamma - s\alpha c\gamma & c\alpha s\beta c\gamma + s\alpha s\gamma \\ s\alpha c\beta & s\alpha s\beta s\gamma + c\alpha c\gamma & s\alpha s\beta c\gamma - c\alpha s\gamma \\ -s\beta & c\beta s\gamma & c\beta s\gamma \end{bmatrix} \tag{10}$$

where $c*$ and $s*$ are abbreviations for cos$*$ and sin$*$, respectively, and the subscript $\gamma\beta\alpha$ denotes the order of the finite rotations. Furthermore, it is straightforward to show that

$$\boldsymbol{D}_i = {}^1\mathbf{R}^3_{\gamma\beta\alpha}\boldsymbol{D}^*_i + \boldsymbol{r}_{O_3/O_1} \tag{11}$$

where vector $\boldsymbol{D}^*_i$ locates point D_i but expressed in the moving reference frame *xyz*.

After, the lower generalized coordinates $\underline{q}_i$, as well as the coordinates of the points C_i, are obtained by means of Eqs. (1), (2) and (5) whereas the upper generalized coordinates $\overline{q}_i$ are computed by means of Eq. (6).

4. Infinitesimal kinematics

Screw theory has been proved to be an excellent resource to investigate the kinematics of the 3-RPS parallel manipulator, see for instance [22-26], and therefore it is chosen as the mathematical tool to approach the velocity, acceleration and singularity analyses of the series-parallel manipulator.

4.1 Velocity analysis

Let ${}^k\boldsymbol{V}_O^{k+1} = [{}^k\boldsymbol{\omega}^{k+1}; {}^k\boldsymbol{v}_O^{k+1}]^T$ $(k = 1,2)$ be the velocity state of the platform k+1 with respect to the platform k, where ${}^k\boldsymbol{\omega}^{k+1}$ and ${}^k\boldsymbol{v}_O^{k+1}$ are the angular and linear velocities of the platform k+1 taking point O, which is instantaneously coincident with the origin O_1 of the fixed reference frame *XYZ*, as the reference pole. Moreover, the six-dimensional vector ${}^k\boldsymbol{V}_O^{k+1}$ can be written in screw form, the infinitesimal screws are depicted in Fig. 1, as

$${}^k\mathbf{J}_i^{k+1}\,{}^k\Omega_i^{k+1} = {}^k\boldsymbol{V}_O^{k+1} \tag{12}$$

where ${}^k\mathbf{J}_i^{k+1}$ and ${}^k\Omega_i^{k+1}$ are, respectively, the screw-coordinate Jacobian matrix and the joint-rate velocity matrix of the indicated limb. For the LPM k= 1 and ${}^1\mathbf{J}_i^2 = [{}^0\underline{\$}_i^1 \;\; {}^1\underline{\$}_i^2 \;\; \cdots \;\; {}^5\underline{\$}_i^6]$ while ${}^1\Omega_i^2 = [{}_0\underline{\omega}_1^i \;\; {}_1\underline{\omega}_2^i \;\; \cdots \;\; {}_5\underline{\omega}_6^i]^T$. Similarly, for the UPM k = 2 and ${}^2\mathbf{J}_i^3 = [{}^0\overline{\$}_i^1 \;\; {}^1\overline{\$}_i^2 \;\; \cdots \;\; {}^5\overline{\$}_i^6]$ whereas ${}^2\Omega_i^3 = [{}_0\overline{\omega}_1^i \;\; {}_1\overline{\omega}_2^i \;\; \cdots \;\; {}_5\overline{\omega}_6^i]^T$.

It should be noted that the joint rates ${}_0\underline{\omega}_1^i = \dot{\underline{q}}_i$ and ${}_2\overline{\omega}_3^i = \dot{\overline{q}}_i$ have the privilege to be chosen as the generalized speeds of the robot. Furthermore, the velocity state ${}^1\boldsymbol{V}_O^3$ of the output platform

$${}^1\boldsymbol{V}_O^3 = {}^1\boldsymbol{V}_O^2 + {}^2\boldsymbol{V}_O^3 \tag{13}$$

where ${}^1\boldsymbol{V}_O^2$ is the velocity state of the coupler platform with respect to the fixed platform while ${}^2\boldsymbol{V}_O^3$ is the velocity state between the output and coupler platforms.

The forward velocity analysis is formulated as follows: given the active joint rate velocities of the robot $\{\dot{\underline{q}}_i, \dot{\overline{q}}_i\}$, compute the angular and linear velocities of the center of the output platform. Using reciprocal screw theory [26, 27] the Input/Output equation of velocity between platforms 1 and 2 results in

$$\mathbf{J}_1^T \Delta {}^1\boldsymbol{V}_O^2 = {}^1\dot{\mathbf{Q}}^2 = [\dot{\underline{q}}_1\{{}^4\underline{\$}_1^5;{}^0\underline{\$}_1^1\} \quad \dot{\underline{q}}_2\{{}^4\underline{\$}_2^5;{}^0\underline{\$}_2^1\} \quad \dot{\underline{q}}_3\{{}^4\underline{\$}_3^5;{}^0\underline{\$}_3^1\} \quad 0 \quad 0 \quad 0]^T \tag{14}$$

therein $\mathbf{J}_1 = [{}^4\underline{\$}_1^5 \quad {}^4\underline{\$}_2^5 \quad {}^4\underline{\$}_3^5 \quad {}^5\underline{\$}_1^6 \quad {}^5\underline{\$}_2^6 \quad {}^5\underline{\$}_3^6]$ is the active screw-coordinate Jacobian matrix of the LPM,

$$\Delta = \begin{bmatrix} \mathbf{0} & \mathbf{I} \\ \mathbf{I} & \mathbf{0} \end{bmatrix}$$

is partitioned into 3×3 blocks [28] so that **0** is the zero-matrix and **I** is the identity-matrix, and $\{*;*\}$ denotes the Klein form of the Lie algebra $e(3)$ of the Euclidian group $E(3)$. Similarly, the input/output equation of velocity concerned with the velocity state ${}^2\boldsymbol{V}_O^3$ results in

$$\mathbf{J}_2^T \Delta {}^2\boldsymbol{V}_O^3 = {}^2\dot{\mathbf{Q}}^3 = [\dot{\bar{q}}_1 \quad \dot{\bar{q}}_2 \quad \dot{\bar{q}}_3 \quad 0 \quad 0 \quad 0]^T \tag{15}$$

where $\mathbf{J}_2 = [{}^2\bar{\$}_1^3 \quad {}^2\bar{\$}_2^3 \quad {}^2\bar{\$}_3^3 \quad {}^4\bar{\$}_1^5 \quad {}^4\bar{\$}_2^5 \quad {}^4\bar{\$}_3^5]$ is the active screw-coordinate Jacobian matrix of the UPM. Hence, assuming that the active Jacobian $\mathbf{J}_1$ and $\mathbf{J}_2$ are nonsingular then the velocity states ${}^1\boldsymbol{V}_O^2$ and ${}^2\boldsymbol{V}_O^3$ can be obtained, respectively, by means of Eqs. (14) and (15) while the velocity state ${}^1\boldsymbol{V}_O^3$ is computed from Eq. (13). On the other hand, the inverse velocity analysis consists of finding the generalized joint-rate velocities for a prescribed velocity state ${}^1\boldsymbol{V}_O^3$. This analysis is carried-out by means of Eqs. (13)-(15). Furthermore, with these expressions it is possible to write a linear relationship between the input joint-rate velocities and the desired velocity ${}^1\boldsymbol{V}_O^3$ as

$$[\mathbf{J}_1^T\Delta]^{-1}\, {}^1\dot{\mathbf{Q}}^2 + [\mathbf{J}_2^T\Delta]^{-1}\, {}^2\dot{\mathbf{Q}}^3 = {}^1\boldsymbol{V}_O^3 . \tag{16}$$

4.2 Acceleration analysis

Let ${}^k\boldsymbol{A}_O^{k+1} = [{}^k\dot{\boldsymbol{\omega}}^{k+1};{}^k\boldsymbol{a}_O^{k+1} - {}^k\boldsymbol{\omega}_O^{k+1} \times {}^k\boldsymbol{v}_O^{k+1}]^T$ $(k = 1, 2)$ be the reduced acceleration state of the platform k+1 with respect to platform k, where ${}^k\dot{\boldsymbol{\omega}}^{k+1}$ and ${}^k\boldsymbol{a}_O^{k+1}$ are the angular and linear accelerations of the platform k+1 taking point O as the reference pole. Furthermore, the six-dimensional vector ${}^k\boldsymbol{A}_O^{k+1}$ can be written in screw form [29] as

$${}^k\mathbf{J}_i^{k+1}\, {}^k\dot{\Omega}_i^{k+1} + {}^k\mathcal{L}_i^{k+1} = {}^k\boldsymbol{A}_O^{k+1} \tag{17}$$

where ${}^k\dot{\Omega}_i^{k+1}$ is the joint-rate acceleration matrix of the indicated limb, ${}^k\dot{\Omega}_i^{k+1} = \frac{d}{dt}\, {}^k\Omega_i^{k+1}$, and ${}^k\mathcal{L}_i^{k+1}$ is the Lie screw which is calculated as

$$\mathcal{L}_i = \sum_{j=0}^{4} [\, {}_j\omega_{j+1}^i\, {}^j\$_i^{j+1} \quad \sum_{k=j+1}^{5} {}_k\omega_{k+1}^i\, {}^k\$_i^{k+1}] \tag{18}$$

where the brackets $[* \quad *]$ denote the Lie product of the Lie algebra $e(3)$ of the Euclidian group $E(3)$. Naturally, underlines and overlines make the difference between the Lie screws of the upper and lower manipulators. Furthermore, the reduced acceleration state ${}^1\boldsymbol{A}_O^3$ of the output platform with respect to the fixed platform can be written as

$${}^1\boldsymbol{A}_O^3 = {}^1\boldsymbol{A}_O^2 + {}^2\boldsymbol{A}_O^3 + [{}^1\boldsymbol{V}_O^2 \quad {}^2\boldsymbol{V}_O^3] \tag{19}$$

where ${}^1\boldsymbol{A}_O^2$ is the reduced acceleration state of the coupler platform with respect to the fixed platform while ${}^2\boldsymbol{A}_O^3$ is the reduced acceleration state between the output and coupler platforms.

The forward acceleration analysis is formulated as follows: given the active joint-rate accelerations $\{\ddot{\underline{q}}_i, \ddot{\bar{q}}_i\}$, compute the angular and linear accelerations of the center of the moving platform. Following the trend of the velocity analysis, the Input/Output equations of acceleration of the series-parallel manipulator result in

$$\left.\begin{array}{l} \mathbf{J}_1^T\Delta\, {}^1\boldsymbol{A}_O^2 = {}^1\ddot{\mathbf{Q}}^2 = \begin{bmatrix} \{{}^4\underline{\$}_1^5;\ddot{\underline{q}}_1\, {}^0\underline{\$}_1^1 + \underline{\mathcal{L}}_1\} \\ \{{}^4\underline{\$}_2^5;\ddot{\underline{q}}_2\, {}^0\underline{\$}_2^1 + \underline{\mathcal{L}}_2\} \\ \{{}^4\underline{\$}_3^5;\ddot{\underline{q}}_3\, {}^0\underline{\$}_3^1 + \underline{\mathcal{L}}_3\} \\ \{{}^5\underline{\$}_1^6;\underline{\mathcal{L}}_1\} \\ \{{}^5\underline{\$}_2^6;\underline{\mathcal{L}}_2\} \\ \{{}^5\underline{\$}_3^6;\underline{\mathcal{L}}_3\} \end{bmatrix} \\ \mathbf{J}_2^T\Delta\, {}^2\boldsymbol{A}_O^3 = {}^2\ddot{\mathbf{Q}}^3 = \begin{bmatrix} \ddot{\bar{q}}_1 + \{{}^4\bar{\$}_1^5;\bar{\mathcal{L}}_1\} \\ \ddot{\bar{q}}_2 + \{{}^4\bar{\$}_2^5;\bar{\mathcal{L}}_2\} \\ \ddot{\bar{q}}_3 + \{{}^4\bar{\$}_3^5;\bar{\mathcal{L}}_3\} \\ \{{}^5\bar{\$}_1^6;\bar{\mathcal{L}}_1\} \\ \{{}^5\bar{\$}_2^6;\bar{\mathcal{L}}_2\} \\ \{{}^5\bar{\$}_3^6;\bar{\mathcal{L}}_3\} \end{bmatrix} \end{array}\right\} . \tag{20}$$

Hence, the reduced acceleration states ${}^1\boldsymbol{A}_O^2$ and ${}^2\boldsymbol{A}_O^3$ are obtained through Eq. (20) while the reduced acceleration state of the output platform with respect to the fixed platform, ${}^1\boldsymbol{A}_O^3$, is computed from Eq. (19). Once the six-dimensional vector ${}^1\boldsymbol{A}_O^3$ is determined, the linear velocity and accelerations of point O are calculated by applying the concept of helicoidal vector field [30]. Finally, in order to solve the inverse acceleration analysis, or in other words with the purpose to compute the active joint-rate accelerations of the robot, from Eqs. (19)-(20) it is possible to establish a linear relationship between the required joint-rate accelerations and the prescribed reduced acceleration state ${}^{1}\boldsymbol{A}_O^3$ as follows:

$$[\mathbf{J}_1^T\boldsymbol{\Delta}]^{-1}\, {}^{1}\ddot{\mathbf{Q}}^2 + [\mathbf{J}_2^T\boldsymbol{\Delta}]^{-1}\, {}^{2}\ddot{\mathbf{Q}}^3 + [{}^{1}\boldsymbol{V}_O^2 \quad {}^{2}\boldsymbol{V}_O^3] = {}^{1}\boldsymbol{A}_O^3 \tag{21}$$

4.3 Singularity analysis

The singularity analysis of the tangential 3-RPS parallel manipulator has been deeply investigated and therefore the singularity analysis here reported is devoted only to the LPM. To this aim Eq. (14) is rewritten as

$$\mathbf{A}\boldsymbol{V}_O = \mathbf{B}\dot{\mathbf{q}} \tag{22}$$

where $\mathbf{A} = \mathbf{J}_1^T\,\boldsymbol{\Delta}$, $\dot{\mathbf{q}} = [\dot{q}_1 \quad \dot{q}_2 \quad \dot{q}_3 \quad 0 \quad 0 \quad 0]^T$ and

$$\mathbf{B} = \begin{bmatrix} \{{}^{4}\underline{\$}_1^5; {}^{0}\underline{\$}_1^1\} & 0 & 0 & 0 & 0 & 0 \\ 0 & \{{}^{4}\underline{\$}_2^5; {}^{0}\underline{\$}_2^1\} & 0 & 0 & 0 & 0 \\ 0 & 0 & \{{}^{4}\underline{\$}_3^5; {}^{0}\underline{\$}_3^1\} & 0 & 0 & 0 \\ 0 & 0 & 0 & 1 & 0 & 0 \\ 0 & 0 & 0 & 0 & 1 & 0 \\ 0 & 0 & 0 & 0 & 0 & 1 \end{bmatrix}. \tag{23}$$

According to Eq. (22) a singular configuration emerges when: i) matrix **A** is singular, namely singularity type 2 ii) matrix **B** is singular, namely singularity type 1 iii) **A** and **B** are both singular, namely singularity type 3. For details the reader is referred to Gosselin and Angeles [31].

Singularity type 2 is concerned with the forward kinematics of the robot. It is evident that matrix **A** is singular when the active Jacobian matrix $\mathbf{J}_1$ is singular. Hence, in order to investigate singularities type 2, the active Jacobian $\mathbf{J}_1$ is recalled here:

$$\mathbf{J}_1 = [{}^{4}\underline{\$}_1^5 \quad {}^{4}\underline{\$}_2^5 \quad {}^{4}\underline{\$}_3^5 \quad {}^{5}\underline{\$}_1^6 \quad {}^{5}\underline{\$}_2^6 \quad {}^{5}\underline{\$}_3^6]. \tag{24}$$

The detection of this type of singularity can be achieved by analyzing the dimension of matrix $\mathbf{J}_1$, clearly when $\dim(\mathbf{J}_1)<6$. Consider for instance that if the elements of $\mathbf{J}_1$ are coplanar or concurrent then the rank of matrix $\mathbf{J}_1$ becomes deficient, however both situations, owing to topology of the LPM, are impossible because the screws $\{{}^{4}\underline{\$}_1^5, {}^{4}\underline{\$}_2^5, {}^{4}\underline{\$}_3^5,\}$ cannot be concurrent due to the tangential arrangement of the lower links and the screws $\{{}^{5}\underline{\$}_1^6, {}^{5}\underline{\$}_2^6, {}^{5}\underline{\$}_3^6,\}$ cannot be evidently coplanar due to the inclined angle Θ. Furthermore, if $\boldsymbol{d}_i = \boldsymbol{d}_j$, $i, j = 1, 2, 3$, in other words if there are physical interferences between the lower links, then ${}^{4}\underline{\$}_i^5 = {}^{4}\underline{\$}_j^5$ and ${}^{5}\underline{\$}_1^6 = {}^{5}\underline{\$}_2^6$ causing the singularity of the LPM. It is worth to note that if matrix **A** is singular, then det(**A**) = 0 which implies that the velocity state $\boldsymbol{V}_O$ admits arbitrary values, and therefore the motions of the coupler platform are uncontrollable. In fact, provided that det(**A**) = 0 and det(**B**) ≠ 0, there is not a one by one mapping, see Eq. (22), between the velocity state $\boldsymbol{V}_O$ and the matrix $\dot{\mathbf{q}}$. On the other hand, the singularity analysis in loci form, also known as the *illness regions* of the manipulator, can be achieved taking into account that det(**A**) = 0, however due to the lack of an exact solution concerned with the forward displacement analysis, the symbolic computation of such determinant is a hazardous task that is beyond the purpose of the contribution, a numerical approach is a viable option to compute the singular surfaces, if any.

Singularity type 1 occurs when det(**B**) = 0. This undesirable situation emerges when any of the elements of the diagonal of the matrix **B** vanishes, in other words when the screws ${}^{4}\underline{\$}_i^5$ and ${}^{0}\underline{\$}_i^1$, of course in the same limb, are reciprocal yielding $\{{}^{4}\underline{\$}_i^5; {}^{0}\underline{\$}_i^1\} = 0$. The only possibility is present when any of three points C_i is located on the Y axis.

Finally, if the vectors $\boldsymbol{d}_i$ are parallel, the screws ${}^{4}\underline{\$}_i^5$ are coplanar, and point C_1 is located on the Y axis, then det(**A**) = det(**B**) = 0 and the LPM is at a singular configuration type 3. However, due to the fact that the lower links are constrained to rotate about the same axis, then this possibility can be disregarded immediately.

5. Case study

In this section a numerical example is provided. Using hereafter SI units, the parameters of the robot are chosen as $h = 0.19$, $r = 0.5$, $\Theta = 0.7854$, $e = 0.433$ and $g = 0.2165$. With these data the characteristic equations of the LPM result in

$$\begin{aligned} &(0.7071\, d_i + 0.7071\, d_j - d_i d_j - 0.5)\cos(q_i - q_j) + d_i^2 + d_j^2 \\ &-d_i d_j - 0.7071\, d_i - 0.7071\, d_j + 0.3125 = 0 \\ &\qquad\qquad i, j = 1, 2, 3 \quad \text{mod}(3)\,. \end{aligned} \tag{25}$$

With the purpose to show that the LPM is practically free of singularities, a Maple©sheet was implemented in order to compute the determinant of the active Jacobian matrix $\mathbf{J}_1$. To this aim, the ranges of the lower generalized coordinates are selected as $\pi/2 \le \underline{q}_1 \le 3\pi/2$, $6\pi/7 \le \underline{q}_2 \le 4\pi/3$, and $11\pi/6 \le \underline{q}_3 \le 2\pi$. The numerical results obtained with computer code confirm that none of the calculated determinants vanishes.

The next part of the case study is concerned with inverse kinematics of the robot. To this end, consider that the center of the output platform is commanded to move according to an imposed trajectory given by

$$\boldsymbol{r}_{O_3/O_1} = -0.15\sin(t)\hat{i} + 0.5\sin(t)\cos^2(t)\hat{j} + 0.25\sin(t)\hat{k}$$

whereas the instantaneous angles of the rotation matrix are selected as $\gamma = \Theta_X = 0.5\sin^2(t), \beta = \Theta_Y = -0.1\sin(t)$ and $\alpha = \Theta_Z = 0.25\sin(t)\cos(t)$. After, in order to satisfy this task,

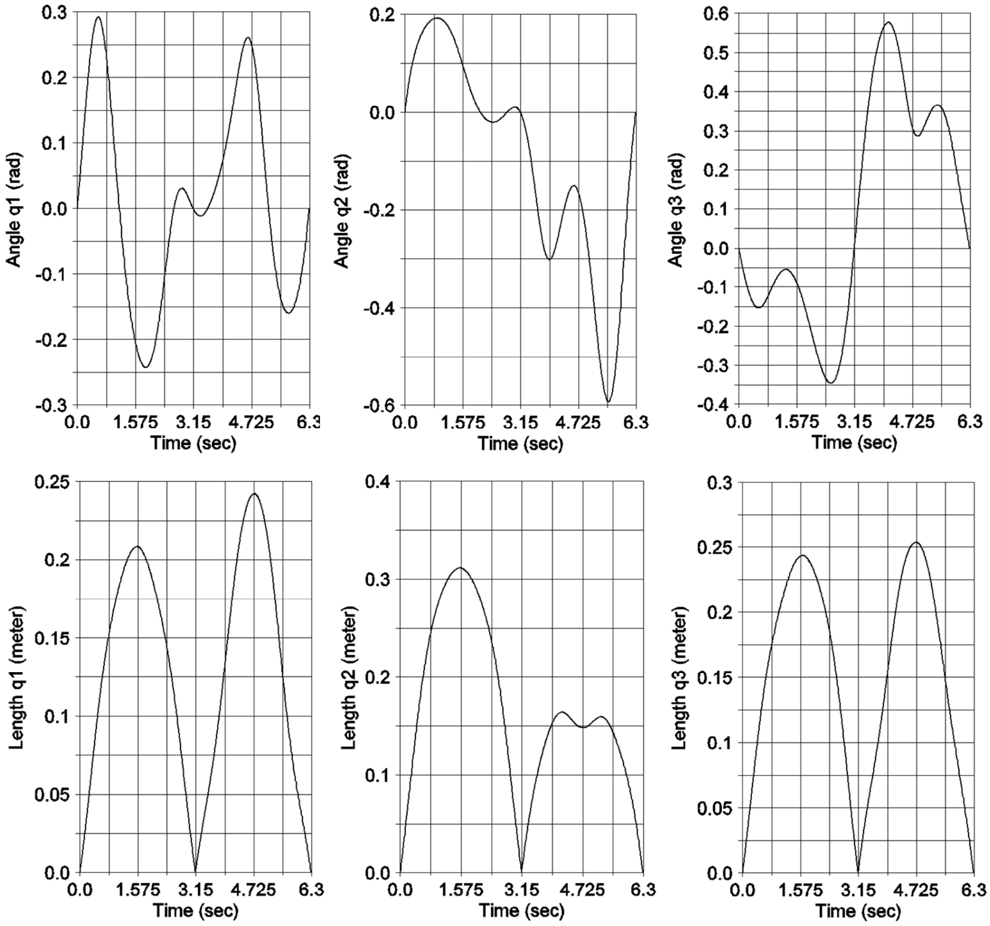

Fig. 2. Time history of the fluctuations of the generalized coordinates.

the required fluctuation of the generalized coordinates $\underline{q}_i$ and $\overline{q}_i$ are given, respectively, in Fig. 2.

The final part of the case study deals with the forward kinematics of the robot. Assuming that the generalized coordinates are governed by periodical functions given by

$$\underline{q}_1 = 1.5708 - 0.25\sin(t),\ \underline{q}_2 = 3.6652 + 0.125\sin(t),$$
$$\underline{q}_3 = 5.7596 - 0.4\sin(t),\ \overline{q}_1 = 0.4574 + 0.1\sin(t),$$
$$\overline{q}_2 = 0.4574 + 0.05\sin(t),\ \overline{q}_3 = 0.4574 + 0.1\sin(t)$$

where the interval for the time t is given by $0 < t < 2\pi$, the exercise consists of finding the angular and linear kinematic properties of the center of the output platform up to the acceleration analysis. These results are shown in Fig. 3. Furthermore, the numerical results obtained via screw theory are compared with simulations generated with the aid of special software like ADAMS©.

6. Discussion

A typical 2(3-RPS) series parallel robot consists of two 3-RPS parallel manipulators assembled in series connection having triangular and hexagonal moving platforms. It is evident that this manipulator possess important benefit such as better workspace and manipulability when it is compared with the 3-RPS parallel manipulator, however exhibits the following limitations: i) the mobility should be reconsidered due to the fact that the orientation of the output platform cannot be arbitrary with respect to the coupler platform. A similar restriction exists between the coupler and fixed platforms ii) the combination of triangular and hexagonal platforms requires the introduction of several parameters in order to approach the displacement analysis iii) the bending moments acting on the coupler platform can affect the accuracy of the mechanism. Perhaps, the most critical of these drawbacks is concerned with the mobility of the robot. Although the Chebichev-Kutzbach-Grübler criterion indicates that the 2(3-RPS) series-parallel manipulator is capable to realize six degrees of freedom, it should be noted that Dai et al. [8] proved that in a 3-RPS tangential parallel manipulator a basis representing the motions of the moving platform, with respect to the fixed platform, consists of three elements, two nonparallel coplanar rotations, and one translation along an axis normal to the plane of the moving platform. According to this basis, the platform 2 of the robot cannot rotate with respect to the platform 1

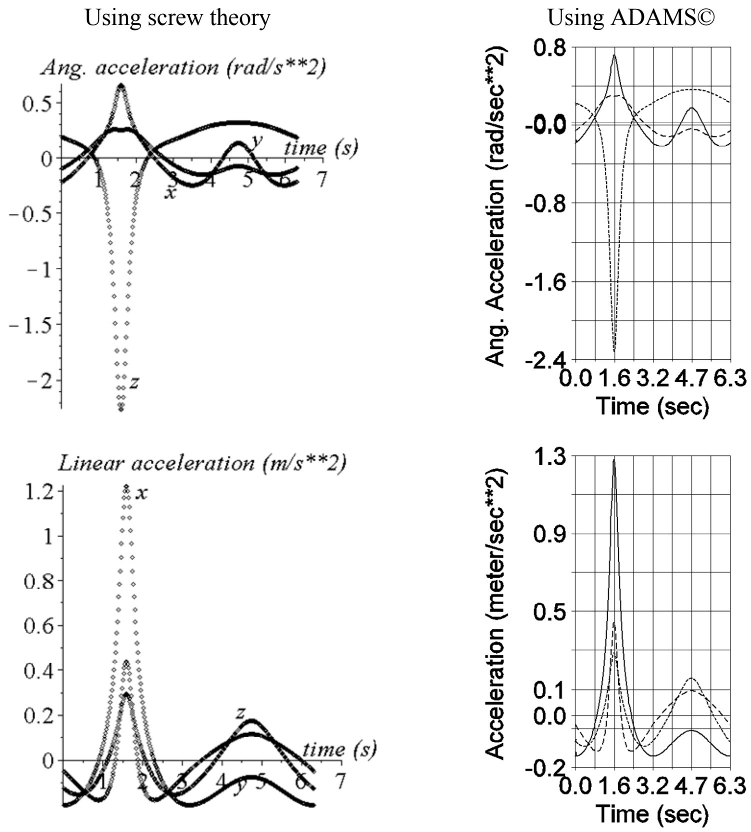

Fig. 3. Time history of the forward kinematics of the center of the moving platform.

along an axis normal to the plane of the coupler platform. It is straightforward to demonstrate that such argument is also valid for the platforms 3 and 2. In fact, the output platform has one rotation restricted with respect to the coupler platform.

Certainly, since the angular velocity vector of the output platform, with respect to the fixed platform, can be obtained through the coupler platform as the vector sum ${}^1\boldsymbol{\omega}^3 = {}^1\boldsymbol{\omega}^2 + {}^2\boldsymbol{\omega}^3$, where the vectors ${}^1\boldsymbol{\omega}^2$ and ${}^2\boldsymbol{\omega}^3$ are located, respectively, in the planes of the coupler and output platforms, in a glance a natural assumption is that the vector ${}^1\boldsymbol{\omega}^3$ can be arbitrary dealing with the inverse kinematics of the robot, excepting the case where the planes of the output and coupler platforms are parallel. However, it must be noted that given an arbitrary pose of the output platform with respect to the fixed platform, the pose of the coupler platform cannot be arbitrary due to the constraints imposed by the revolute joints. In fact, there at most eight distinct poses of the coupler platform given the pose of the output platform.

Concluding this section, in a classical 2(3-RPS) series-parallel manipulator the output platform can perform a desired orientation if: i) the coupler platform can reach one of the eight available poses associated to the inverse position analysis, of course imaginary and singular solutions are disregarded ii) the motion of the output platform does not produce rotations normal to the planes of the output and coupler platforms. If any of these conditions is not fulfilled, the required motion of the output platform cannot be achieved by the robot.

7. Conclusions

In this work a series-parallel manipulator capable to realize six degrees of freedom in the general Cartesian task space is introduced. Unlike the 2(3-RPS) robot, the manipulator here proposed admits arbitrary orientations of the output platform with respect to the fixed platform. The lower mechanism is a 3-PPS parallel manipulator where the kinematic pairs connecting the limbs to the fixed platform are prismatic joints moving on circular trajectories about the center of the fixed platform while the PS-type limbs are inclined kinematic chains where the lines along the limbs intersect a common point. These characteristics allow the coupler platform to reach arbitrary orientations, followed by parasitic translations, with respect to the fixed platform. On the other hand, the upper parallel manipulator is a tangential 3-RPS parallel manipulator in which the output platform can reach arbitrary positions, followed by parasitic orientations, with respect to the coupler platform. The result of connecting a *spherical parallel manipulator with parasitic translations* with a *translational parallel manipulator with parasitic rotations* is a non-redundant six degrees-of-freedom series-parallel manipulator. In fact, in the proposed robot the orientation and position of the output platform, with respect to the fixed platform, are controlled, respectively, by means of the lower and upper parallel manipulators and therefore the proposed robot belongs to the class known as robots with decoupled kinematics. As far as the authors are aware, this type of series-parallel manipulator has not been considered in previous works, even though the 3-RPS parallel manipulator was introduced almost three decades ago.

In order to show the performance of the proposed robot, a case study was included. The numerical example covered the following subjects of the kinematic analysis: i) computation of the characteristic equations ii) detection of singularities type 2 in the lower parallel manipulator using a numerical approach. The numerical results of this point ensure that the case study is free of singularities associated with the forward kinematics, all the solutions of the forward displacement analysis were taken into account iii) dealing with the inverse kinematics, the most interesting characteristic of the robot, several arbitrary poses, positions and orientations in the form of periodical functions, were assigned to the output platform and in all the cases the robot can fulfill the required tasks. Only one of these cases is explained in section 5 iv) with the purpose to exemplify the forward kinematics, periodical functions were assigned to the generalized coordinates in order to compute the angular and linear kinematic properties of the center of the output platform. Furthermore, these results were successfully compared with simulations generated with the aid of special software like ADAMS©.

Finally, the virtual model realized with ADAMS© shows that the workspace of the series-parallel manipulator is limited only by the possible mechanical interference between the links of the robot.

Acknowledgment

This work was supported by DGEST and Conacyt of México.

References

[1] M. Zoppi, D. Zlatanov and R. Molfino, On the velocity analysis of interconnected chains mechanisms, *Mech. Mach. Theory*, 41 (2006) 1346-1358.

[2] V. E. Gough and S. G. Whitehall, Universal tire testing machine, *Proc. of the FISITA Ninth International Technical Congress, IMechE 1* (1962) 117-137.

[3] C. Innocenti, Forward kinematics in polynomial form of the general Stewart platform, *ASME J. Mech. Des*., 123 (2001) 254-260.

[4] L. Rolland, Certified solving of the forward kinematics problem with an exact algebraic method for the general parallel manipulator, *Adv. Robotics*, 19 (2005) 995-1025.

[5] J. Gallardo-Alvarado, C. R. Aguilar-Nájera, L. Casique-Rosas, J. M. Rico-Martínez and Md. Nazrul Islam, Kinematics and dynamics of 2(3-RPS) manipulators by means of screw theory and the principle of virtual work, *Mech. Mach. Theory*, 43 (2008) 1281-1294.

[6] I. A. Bonev, *Geometric analysis of parallel mechanisms*, thèse de doctorat, Université Laval, Canada, November (2002).

[7] I. A. Bonev, Direct kinematics of zero-torsion parallel mechanisms, *Proc. IEEE International Conference on Robotics and Automation*, Pasadena, California, USA, May 19-23, 2008.

[8] J. S. Dai, Z. Huang and H. Lipkin, Mobility of overconstrained parallel mechanisms, *ASME J. Mech. Des.* 128 (2006) 220-229.

[9] K. H. Hunt, Structural kinematics of in-parallel actuated robot arms, *ASME J. Mech. Transm. Automat. Des.* 105 (1983) 705-712.

[10] K. J. Waldron, M. Raghavan and B. Roth, Kinematics of a hybrid series-parallel manipulation system, *ASME J. Dyn. Syst. Meas. Control*, 111 (1989) 211-221.

[11] K. M. Lee and S. A. Arjuman, 3-DOF micromotion in-parallel actuated manipulator, *IEEE Trans. Robotics Automat.* 7 (1991) 634-640.

[12] G. H. Pfreundschuh, V. Kumar and T. H. Sugar, Design and control of a three-degree-of-freedom in-parallel actuated manipulator, *Proc. of the IEEE International Conference on Robotics and Automation* (1991) 1659-1664.

[13] Y. G. Li, H. T. Liu, X. M. Zhao, T. Huang and D. Chetwynd, Design of a 3-DOF PKM module for large structural component machining, *Mech. Mach. Theory*, 45 (2010) 941-954.

[14] J. Gallardo-Alvarado, H. Orozco-Mendoza and J. M. Rico-Martínez, A novel five-degrees-of-freedom decoupled robot, *Robotica*, 28 (2010) 909-917.

[15] J. Gallardo-Alvarado, DeLiA: a new redundant partially decoupled robot, *Adv. Robotics*, 25 (2011) 1295-1310.

[16] Y. Lu and T. Leinonen, Solution and simulation of position-orientation for multi-spatial 3-RPS parallel mechanisms in series connection, *Multibody Syst. Dyn.* 14 (2005) 47-60.

[17] J. Gallardo-Alvarado, C. R. Aguilar-Nájera, L. Casique-Rosas, L. Pérez-González and J. M. Rico-Martínez, Solving the kinematics and dynamics of a modular spatial hyper-redundant manipulator by means of screw theory, *Multibody Syst. Dyn.* 20 (2008) 307-325.

[18] Y. Lu, B. Hu and T. Sun, Analyses of velocity, acceleration, statics, and workspace of a 2(3-SPR) serial-parallel manipulator, *Robotica*, 27 (2009) 529-538.

[19] G. Gogu, Mobility of mechanisms: a critical review, *Mech. Mach. Theory*, 40 (2005) 1068-1097.

[20] R. I. Alizade, N. R. Tagiyev and J. Duffy, A forward and reverse displacement analysis of a 6-DOF in-parallel manipulator, *Mech. Mach. Theory*, 29 (1994) 115-124.

[21] C. Innocenti and V. Parenti-Castelli, Direct position analysis of the Stewart platform mechanism, *Mech. Mach. Theory*, 35 (1990) 611-621.

[22] S. K. Agrawal, Study of an in-parallel mechanism using reciprocal screws, *Proc. of the 8-th World Congress on TMM* (1991) 405-408.

[23] Z. Huang and Y. F. Fang, Kinematic characteristics analysis of 3 DOF in-parallel actuated pyramid mechanism, *Mech. Mach. Theory*, 31 (1996) 1009-1018.

[24] Z. Huang and J. Wang, Identification of principal screws of

3-DOF parallel manipulators by quadric degeneration, *Mech. Mach. Theory,* 16 (2001) 893-911.
[25] Z. Huang, J. Wang and Y. F. Fang, Analysis of instantaneous motions of deficient-rank 3-RPS parallel manipulators, *Mech. Mach. Theory*, 37 (2002) 229-240.
[26] J. Gallardo, H. Orozco and J. M. Rico, Kinematics of 3-RPS parallel manipulators by means of screw theory, *Int. J. Adv. Manufact. Tech.* 36 (2008) 598-605.
[27] J. M. Rico-Martínez and J. Duffy, Forward and inverse acceleration analyses of in-parallel manipulators, *ASME J. Mech. Des.* 122 (2000) 299-303.
[28] H. Lipkin and J. Duffy, The elliptic polarity of screws, *ASME J. Mech. Transm. Automat. Des.* 107 (1985) 377-388.
[29] J. M. Rico and J. Duffy, An application of screw algebra to the acceleration analysis of serial chains, *Mech. Mach. Theory*, 31 (1996) 445-457.
[30] J. Gallardo-Alvarado, H. Orozco-Mendoza and R. Rodríguez-Castro, Finding the jerk properties of multibody systems using helicoidal vector fields, *Inst. Mech. Engrs. Part C: J. Mech. Eng. Sci.,* 222 (2008) 2217-2229.
[31] C. Gosselin and J. Angeles, Singularity analysis of closed-loop kinematic chains, *IEEE Trans. Robotics & Autom.,* 6 (1990) 261-290.

J. Gallardo-Alvarado is native of Cerro Gordo, GTO, México. He received the BSc and MSc degrees in mechanical engineering from Instituto Tecnológico de Celaya, México, in 1985 and 1988 respectively; and the Ph.D in electrical engineering from Instituto Tecnológico de la Laguna, México, in 1999. He had authored more than 30 journal papers and his interests cover spatial kinematics and dynamics of robotics systems using screw theory. Dr. Gallardo is a current full time professor at the Department of Mechanical Engineering of the Instituto Tecnológico de Celaya and He is a member of the National System of Researchers of México.

R. Rodríguez-Castro is native of Celaya, GTO, México. He obtained a BSc degree in mechanical engineering from Instituto Tecnológico de Celaya, and a MSc in applied mechanics from the Instituto Tecnológico de Querétaro, in 1986 and 1989, respectively; and a Ph.D in mechanical engineering from State University of New York-Buffalo in 1999. His current research interests include analysis and control of flexible structures and mechanisms. Dr. Rodríguez is a current full time Professor at the Department of Mechanical Engineering of the Instituto Tecnológico de Celaya, México.

C. R. Aguilar-Nájera is native of Celaya, GTO, México. He obtained a BSc degree in mechanical engineering from Instituto Tecnológico de Celaya in 1979 and a M.Eng in mechanical engineering from the Instituto Tecnológico y de Estudios Superiores de Monterrey in 1985. His main current interests covers mechanical design and experimental mechanics. M.Eng Aguilar is a current full time Professor at the Department of Mechanical Engineering of the Instituto Tecnológico de Celaya, México.

L. Pérez-González is native of Celaya, GTO, México. He obtained a BSc degree in mechanical engineering from Instituto Tecnológico de Celaya in 1979 and a M.Eng in mechanical engineering from the Instituto Tecnológico y de Estudios Superiores de Monterrey in 1981. His current interests covers kinematics and dynamics of multibody systems. M.Eng Pérez is a current full time Professor at the Department of Mechanical Engineering of the Instituto Tecnológico de Celaya, México.